J|A|C|S ARTICLES

Published on Web 09/10/2009

Accurate Determination of Order Parameters from $^{1}H,^{15}N$ Dipolar Couplings in MAS Solid-State NMR Experiments

Veniamin Chevelkov,[†] Uwe Fink,[†] and Bernd Reif*[,†,‡]

Leibniz-Forschungsinstitut für Molekulare Pharmakologie (FMP), Robert-Rössle-Strasse 10, D-13125 Berlin, Germany, and Charité Universitätsmedizin, D-10115 Berlin, Germany

Received April 3, 2009; E-mail: reif@fmp-berlin.de

Abstract: A reliable site-specific estimate of the individual N−H bond lengths in the protein backbone is the fundamental basis of any relaxation experiment in solution and in the solid-state NMR. The N−H bond length can in principle be influenced by hydrogen bonding, which would result in an increased N−H distance. At the same time, dynamics in the backbone induces a reduction of the experimental dipolar coupling due to motional averaging. We present a 3D dipolar recoupling experiment in which the $^{1}H,^{15}N$ dipolar coupling is reintroduced in the indirect dimension using phase-inverted CP to eliminate effects from rf inhomogeneity. We find no variation of the N−H dipolar coupling as a function of hydrogen bonding. Instead, variations in the $^{1}H,^{15}N$ dipolar coupling seem to be due to dynamics of the protein backbone. This is supported by the observed correlation between the $H^{N}-N$ dipolar coupling and the amide proton chemical shift. The experiment is demonstrated for a perdeuterated sample of the α-spectrin SH3 domain. Perdeuteration is a prerequisite to achieve high accuracy. The average error in the analysis of the H−N dipolar couplings is on the order of ±370 Hz (±0.012 Å) and can be as small as 150 Hz, corresponding to a variation of the bond length of ±0.005 Å.

Introduction

Analysis of solution-state and solid-state NMR relaxation data relies on a highly accurate determination of amide proton−nitrogen bond lengths. Even small site-specific variations of the $N-H^{N}$ bond length upon hydrogen bonding, for example, would severely perturb the analysis, as the relaxation rate depends inversely proportional on the sixth power of the distance between the nitrogen and its directly bonded proton. Neutron diffraction studies would in principle be ideally suited to address this question. These data are, however, only available for single crystals of amino acid-derived small compounds[1] and more recently for a few proteins.[2] Recently, N−H bond lengths were measured in solution-state NMR spectroscopy to very high accuracy, yielding values for the averaged N−H bond length in the order of $\bar{r}_{NH} = \langle r_{NH}^{-3}\rangle^{-1/3} = 1.015 \pm 0.006$ Å.[3,4] This value includes the zero-point anharmonic averaging due to N−H bond stretching. A slightly longer value of $\bar{r}_{NH} = 1.041$ Å is obtained when all fast vibrations and librations are absorbed into the effective bond length.[5] This approach requires the measurement of several RDC data sets and yields only the average bond length for all amide sites in the protein. If the data set is sufficiently large, in addition site-specific order parameters can be extracted from the RDC data.[6−9]

Alternatively, highly accurate bond length information can be extracted from MAS solid-state NMR experiments as the dipolar interaction between two spin-1/2 nuclei depends crucially on the distance between the involved spins.[10] In contrast to solution-state NMR, solid-state NMR enables the site-specific analysis of all residues in a single experiment. In the past, quite a number of experiments have been suggested to characterize bond lengths using MAS solid-state NMR.[11−15] On the other hand, the same dipolar couplings are employed to characterize the overall order parameter of local dynamics in the solid state. Experimentally, the two effects cannot easily be separated from another in case no additional information is included in the analysis. Studies of dynamic processes in the solid state have attracted much attention recently. In particular, site-specific order

[†] FMP.
[‡] Charité Universitätsmedizin.

(1) Kvick, A.; Alkaraghouli, A. R.; Koetzle, T. F. *Acta Crystallogr., Sect. B* **1977**, *33*, 3796–3801.
(2) Blakeley, M. P.; Langan, P.; Niimura, N.; Podjarny, A. *Curr. Opin. Struct. Biol.* **2008**, *18*, 593–600.
(3) Ottiger, M.; Bax, A. *J. Am. Chem. Soc.* **1998**, *120*, 12334–12341.
(4) Yao, L.; Vögeli, B.; Ying, J.; Bax, A. *J. Am. Chem. Soc.* **2008**, *130*, 16518–16520.
(5) Vögeli, B.; Yao, L. *J. Am. Chem. Soc.* **2009**, *131*, 3668–3678.
(6) Meiler, J.; Prompers, J. J.; Peti, W.; Griesinger, C.; Bruschweiler, R. *J. Am. Chem. Soc.* **2001**, *123*, 6098–6107.
(7) Peti, W.; Meiler, J.; Brüschweiler, R.; Griesinger, C. *J. Am. Chem. Soc.* **2002**, *124*, 5822–5833.
(8) Tolman, J. R. *J. Am. Chem. Soc.* **2002**, *124*, 12020–12030.
(9) Briggman, K. B.; Tolman, J. R. *J. Am. Chem. Soc.* **2003**, *125*, 10164–10165.
(10) Schmidt-Rohr, K.; Spiess, H. W. *Multidimensional Solid-State NMR and Polymers*; Academic Press: London, 1994.
(11) Munowitz, M. G.; Griffin, R. G.; Bodenhausen, G.; Huang, T. H. *J. Am. Chem. Soc.* **1981**, *103*, 2529–2533.
(12) Hohwy, M.; Jaroniec, C. P.; Reif, B.; Rienstra, C. M.; Griffin, R. G. *J. Am. Chem. Soc.* **2000**, *122*, 3218–3219.
(13) Zhao, X.; Sudmeier, J. L.; Bachovchin, W. W.; Levitt, M. H. *J. Am. Chem. Soc.* **2001**, *123*, 11097–11098.
(14) Song, X.-j.; Rienstra, C. M.; McDermott, A. E. *Magn. Reson. Chem.* **2001**, *39*, S30–S36.
(15) Schnell, I.; Saalwachter, K. *J. Am. Chem. Soc.* **2002**, *124*, 10938–10939.

 10.1021/ja902649u CCC: $40.75

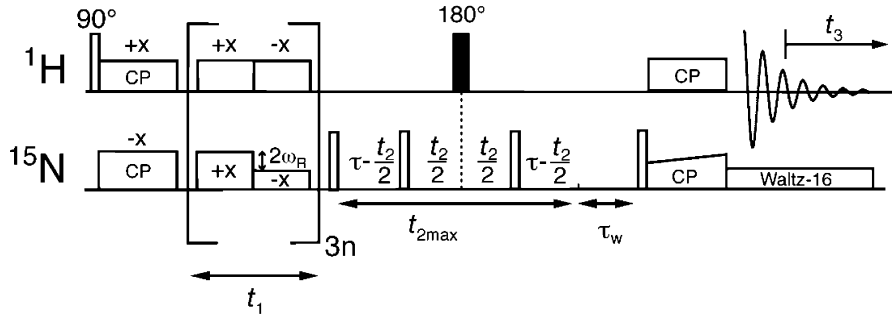

Figure 1. Pulse scheme employed for the measurement of $^1H-^{15}N$ dipolar couplings. Open rectangular bars denote 90° pulses. The $^1H-^{15}N$ dipolar coupling is reintroduced in t_1 using CPPI.[31−33] Heteronuclear scalar decoupling during detection was achieved using WALTZ-16 (ω_{rf} = 2.3 kHz).

parameters were obtained from dipolar recoupling MAS solid-state NMR experiments for various backbone and side chain $^{13}C-^1H$ moieties in the colicin Ia channel,[16] for ubiquitin,[17−19] for intact Pf1 bacteriophage particles,[20] and for a polyalanine repeat fibril sample.[21]

Recently, we suggested a labeling scheme that is based on high levels of deuteration to eliminate most of the undesired proton−proton dipolar interactions.[22,23] In brief, the perdeuterated protein is recrystallized from a buffer containing 90% D_2O to suppress anisotropic interactions among exchangeable sites. Given the fact that high power proton, proton homonuclear decoupling is not required for these samples, N−H dipolar coupling can be quantified with high accuracy. At the same time, possible sources of systematic error (e.g., sample heating) are eliminated. The labeling scheme enables a spin-diffusion free determination of dynamic parameters such as $^{15}N-T_1$,[24−28] heteronuclear Overhauser effects,[29] and $^{15}N-CSA$, $^1H-^{15}N$ dipole cross-correlated relaxation.[30,31] Side chain dynamic information is accessible, making use of the deuterium quadrupolar interaction by interpretation of the spinning sideband manifold.[32−34] $^2H/^{13}C-T_1$ methyl relaxation measurements allow a more detailed characterization of the motional time scale detected in order parameter experiments.[35,36]

In this article, we demonstrate a high-accuracy measurement of $^1H,^{15}N$ dipolar couplings in the backbone of a perdeuterated protein. In protonated samples, the achieved accuracy is in general not satisfactory. Typical errors (e.g., for the protein GB1) are in the order of >±600 Hz for the unscaled $^1H-^{15}N$ dipolar coupling,[17] corresponding to a variation of ±0.02 Å of the bond length. This error is too large to detect reliably site-specific variations of the bond length. Using a perdeuterated sample of the chicken α-spectrin SH3 domain, we show that the error in the determination of dipolar couplings in a phase-inverted CP (CPPI) experiment can be as small as ±150 Hz, corresponding to a variation of the bond length in the order of ca. ±0.005 Å. The average error in the analysis is on the order ±370 Hz (±0.012 Å). In total, we analyzed 48 out of 55 amide backbone groups. Three residues are prolines that do not contain an amide proton, and four residues are located in flexible or disordered regions of the protein and are not visible in our experiments.

Results and Discussion

We employ the pulse scheme represented in Figure 1 to experimentally access the backbone $^1H,^{15}N$ dipolar couplings in the α-spectrin SH3 domain. The scheme relies on the previously introduced CPPI,[37−39] in which the Hartmann−Hahn matching condition alternates between the +1 and −1 rotary resonance condition. CPPI eliminates very efficiently contributions from radio frequency (rf) inhomogeneity (see Supporting Information). In brief, rf inhomogeneity results in an apparently faster dipolar oscillation. A Gaussian distribution of the experimental rf field along the rotor axis would result then in an overestimation of the measured dipolar coupling. At the same time, the error in the determination of the width of the tensor is increased as rf inhomogeneity results in a broadening of the dipolar doublet.

The experimental and simulated dipolar doublets for different residues of the α-spectrin SH3 domain are shown in Figure 2. Variations between the dipolar couplings of residues D14, K18, L61, and D62 are significant. We estimate the uncertainty in the extraction of the experimental dipolar coupling values to

(16) Huster, D.; Xiao, L. S.; Hong, M. *Biochemistry* **2001**, *40*, 7662–7674.
(17) Franks, W. T.; Zhou, D. H.; Wylie, B. J.; Money, B. G.; Graesser, D. T.; Frericks, H. L.; Gurmukh, S.; Rienstra, C. M. *J. Am. Chem. Soc.* **2005**, *127*, 12291–12305.
(18) Lorieau, J. L.; McDermott, A. E. *Magn. Reson. Chem.* **2006**, *44*, 334–347.
(19) Lorieau, J. L.; McDermott, A. E. *J. Am. Chem. Soc.* **2006**, *128*, 11505–11512.
(20) Lorieau, J. L.; Day, L. A.; McDermott, A. E. *Proc. Natl. Acad. Sci. U.S.A.* **2008**, *105*, 10366–10371.
(21) Sackewitz, M.; Scheidt, H. A.; Lodderstedt, G.; Schierhorn, A.; Schwarz, E.; Huster, D. *J. Am. Chem. Soc.* **2008**, *130*, 7172–7173.
(22) Chevelkov, V.; Rehbein, K.; Diehl, A.; Reif, B. *Angew. Chem., Int. Ed.* **2006**, *45*, 3878–3881.
(23) Chevelkov, V.; Reif, B. *Concepts NMR* **2008**, *32A*, 143–156.
(24) Cole, H. B. R.; Torchia, D. A. *Chem. Phys.* **1991**, *158*, 271–281.
(25) Giraud, N.; Böckmann, A.; Lesage, A.; Penin, F.; Blackledge, M.; Emsley, L. *J. Am. Chem. Soc.* **2004**, *126*, 11422–11423.
(26) Giraud, N.; Blackledge, M.; Goldman, M.; Böckmann, A.; Lesage, A.; Penin, F.; Emsley, L. *J. Am. Chem. Soc.* **2005**, *127*, 18190–18201.
(27) Giraud, N.; Blackledge, M.; Böckmann, A.; Emsley, L. *J. Magn. Reson.* **2007**, *184*, 51–61.
(28) Chevelkov, V.; Diehl, A.; Reif, B. *J. Chem. Phys.* **2008**, *128*, 052316.
(29) Giraud, N.; Sein, J.; Pintacuda, G.; Böckmann, A.; Lesage, A.; Blackledge, M.; Emsley, L. *J. Am. Chem. Soc.* **2006**, *128*, 12398–12399.
(30) Chevelkov, V.; Diehl, A.; Reif, B. *Magn. Reson. Chem.* **2007**, *45*, S156–S160.
(31) Skrynnikov, N. R. *Magn. Reson. Chem.* **2007**, *45*, S161–S173.
(32) Hologne, M.; Faelber, K.; Diehl, A.; Reif, B. *J. Am. Chem. Soc.* **2005**, *127*, 11208–11209.
(33) Hologne, M.; Chevelkov, V.; Reif, B. *Prog. Nucl. Magn. Reson. Spectrosc.* **2006**, *48*, 211–232.
(34) Hologne, M.; Chen, Z.; Reif, B. *J. Magn. Reson.* **2006**, *179*, 20–28.
(35) Reif, B.; Xue, Y.; Agarwal, V.; Pavlova, M. S.; Hologne, M.; Diehl, A.; Ryabov, Y. E.; Skrynnikov, N. R. *J. Am. Chem. Soc.* **2006**, *128*, 12354–12355.
(36) Agarwal, V.; Xue, Y.; Skrynnikov, N. R.; Reif, B. *J. Am. Chem. Soc.* **2008**, *130*, 16611–16621.
(37) Wu, X. L.; Zilm, K. W. *J. Magn. Reson., Ser. A* **1993**, *104*, 154–165.
(38) Dvinskikh, S. V.; Zimmermann, H.; Maliniak, A.; Sandstrom, D. *J. Magn. Reson.* **2003**, *164*, 165–170.
(39) Dvinskikh, S. V.; Zimmermann, H.; Maliniak, A.; Sandström, D. *J. Chem. Phys.* **2005**, *122*, 044512.

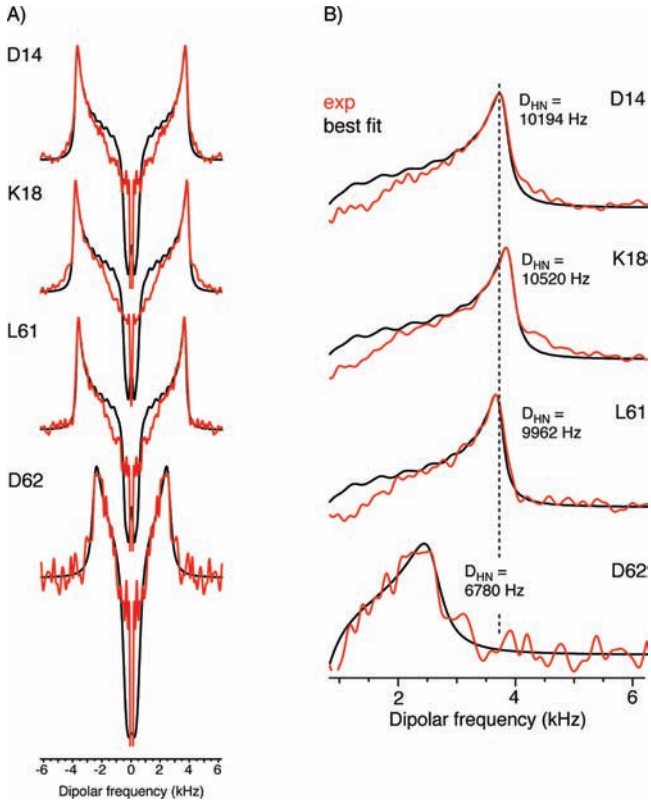

Figure 2. Simulated (black) and experimental (red) $^{1}H,^{15}N$ dipolar frequencies for representative residues in the α-spectrin SH3 domain. (B) Magnification of the right-hand peak of the spectrum shown in (A) maintaining the same scaling. The extracted values for the dipolar coupling tensor are indicated in the figure. The dipolar couplings for all analyzed residues are summarized in the Supporting Information.

be as small as ±50 Hz (see Supporting Information). Other sources of error include possible variations in the size and orientation of the ^{15}N CSA tensor. Fluctuations of this parameter induce a systematic error in the estimation of the true dipolar coupling value which is dominating the total error as discussed in Supporting Information. We approximate this error to be on the order of ±110 Hz for each residue. In the analysis below, the total error comprising sensitivity and line width issues as well as systematic effects from variations of the ^{15}N CSA tensor are taken into account. The extracted $^{1}H,^{15}N$ dipolar couplings together with the error estimation are represented in Figure 3.

The dipolar coupling D_{NH} between a nitrogen and the directly bonded proton is given as

$$D_{NH} = \frac{\mu_0}{4\pi}\frac{\gamma_H \gamma_N \hbar}{r_{NH}^{\ 3}}$$

D_{NH} is dependent on the magnetic permeability μ_0; γ_H and γ_N are the gyromagnetic ratio of the proton and the nitrogen nucleus, respectively; Planck's constant is $\hbar$; and the N−H bond length is r_{NH}. Motion results in averaging of the dipolar coupling D_{NH}, which is described by the order parameter S. The time-averaged order parameter $\langle S \rangle$ is related to[40]

$$\langle S \rangle = \frac{1}{2}\langle 3\cos^2\theta - 1 \rangle = \frac{1}{2}(1 + \cos\theta_0)\cos\theta_0$$

in which θ refers to the angle that the N−H bond vector assumes with respect to its equilibrium position, and θ_0 refers to the half-opening angle of the cone in which the N−H vector diffuses

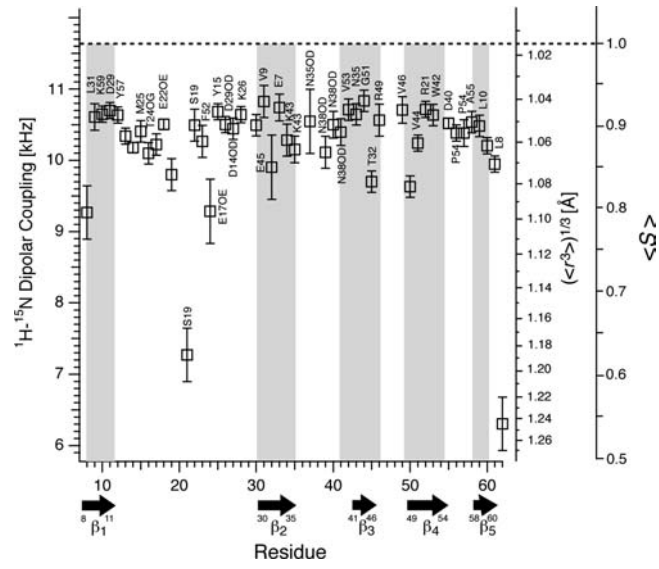

Figure 3. Experimental $^{1}H,^{15}N$ dipolar couplings as a function of residue for the α-spectrin SH3 domain. Assignments indicate the carbonyl hydrogen bonding acceptor of the respective amide proton. The vertical axis on the right-hand side of the figure shows the hypothetical values for the average N−H bond length, $(\langle r^3 \rangle)^{1/3}$ (assuming no motion), and the order parameter $\langle S \rangle$ (assuming no change in the N−H bond length due to hydrogen bonding).

(assuming a diffusion in a cone motion). In this model, an order parameter of $\langle S \rangle = 0.9$ is obtained for a half-opening angle of $\theta_0 = 20°$.

A priori, it is not possible to differentiate if variations in the size of the $^{1}H,^{15}N$ dipolar coupling are due to an increase of the N−H bond length or if they are originating from dynamics in the protein backbone. To appreciate the amplitude of the variation, the experimental values for the average N−H bond length, $(\langle r^3 \rangle)^{1/3}$ assuming no motion, and the order parameter $\langle S \rangle$, assuming no change in the N−H bond length due to hydrogen bonding, are plotted on the right side of the graph (Figure 3). The order parameter $\langle S \rangle$ was set to 1, assuming an effective N−H bond length $(\langle r^3 \rangle)^{1/3}$ of 1.015 Å corresponding to a dipolar coupling of 11 648 Hz (without inclusion of the effects from zero-point librations).[4,5] Most of the N−H order parameters are above 0.9. This is in agreement with the high B-factors of the X-ray structure[41] that shows little side-by-side variation in the protein backbone.

To appreciate the effect of hydrogen bonding, we plotted the size of the $^{1}H-^{15}N$ dipolar couplings as a function of the H^N isotropic chemical shifts (Figure 4). Similar as in solution-state NMR,[42] we would expect a dependence of the strength of the hydrogen bond on the amide proton chemical shift as well as on the size of the dipolar coupling: Strong hydrogen bonds would result in a delocalization of the amide proton and in a elongation of the average N−H bond length. For example, this is observed for one of the imidazole protons in histidine·HCl·H_2O.[13] In case fluctuations of the dipolar couplings are originating from hydrogen bonding, we should observe a decrease in the size of the dipolar coupling for low field shifted amide resonances. We find, however, the opposite behavior. The largest dipolar coupling values are observed for residues with H^N chemical shifts larger than 9.0 ppm.

(40) Lipari, G.; Szabo, A. *J. Chem. Phys.* **1981**, *75*, 2971–2976.
(41) Chevelkov, V.; Faelber, K.; Diehl, A.; Heinemann, U.; Oschkinat, H.; Reif, B. *J. Biomol. NMR* **2005**, *31*, 295–310.
(42) Cordier, F.; Grzesiek, S. *J. Am. Chem. Soc.* **1999**, *121*, 1601–1602.

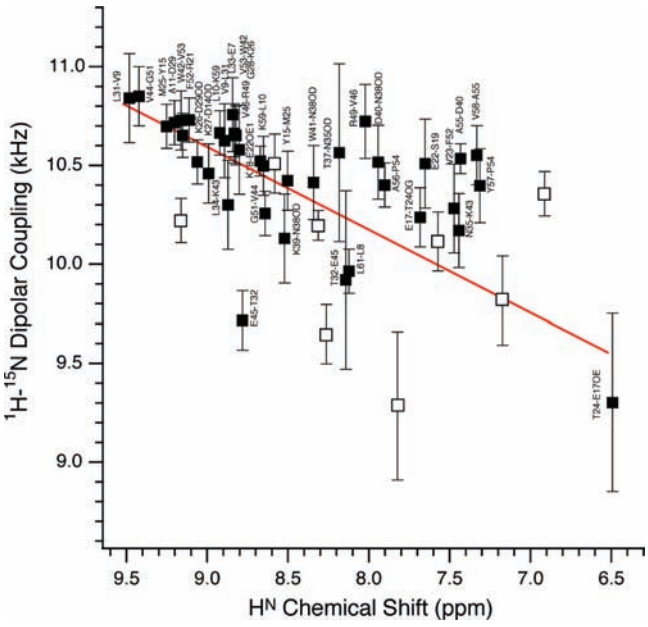

Figure 4. Correlation between the experimental $^1H,^{15}N$ dipolar coupling and the $^1H^N$ isotropic chemical shift. Closed (open) squares represent amides that are found to be involved (not involved) in hydrogen bonds in the X-ray structure. Assignments of the respective hydrogen bonds between an amide proton and its carbonyl/carboxyl acceptor (e.g., $L31H^N-V9C'$) are included in the figure. The linear regression (represented as solid red line) includes only those residues that are involved in hydrogen bonds. A detailed description of the analysis of the error can be found in the Supporting Information.

We interpret this observation by assuming that variations in the size of the $^1H-^{15}N$ dipolar coupling are mostly induced by local dynamics. Residues in the protein that are stabilized by hydrogen bonds exhibit less flexibility and display larger dipolar couplings. By constrast, more flexible parts of the protein in which amide protons are only hydrogen bonded to water will show a decreased amide dipolar coupling. In fact, residues for which no hydrogen bonding partner could be identified in the X-ray structure tend to have smaller dipolar couplings in Figure 3. Obviously, the correlation between the dipolar coupling and the isotropic H^N chemical shifts is very weak. The correlation coefficient for all residues is equal to 0.390 (including D62 and R21). If only residues are taken into account that have dipolar couplings larger than 9500 Hz, the correlation coefficient rises to 0.550. In case T24, L31, and V44 are omitted, the correlation coefficient decreases to 0.380. A similar trend is found if the isotropic chemical shift values are corrected for the amino acid specific average chemical shifts (see Supporting Information). We obtain then a correlation coefficient of 0.505, if all residues are taken into account. In case only β-sheet residues are considered, the correlation coefficient decreases to 0.369. In general, we only observe a modest correlation. However, the positive value of the correlation indicates that the dipolar couplings are decreasing for upfield shifted resonances, which is consistent with the hypothesis that the size of the experimental dipolar couplings are mostly determined by dynamics. This interpretation is in agreement with DFT calculations that predict similar H−N bond lengths for backbone amide protons that are involved in hydrogen bonds either to protein carbonyl groups or to water.[43] The calculated variations in H−N bond lengths are within the error that we report for our measurements. A decrease in dipolar couplings for certain parts of the protein is also consistent with data from complementary relaxation experiments. Residues with largely reduced $^1H-^{15}N$ dipolar coupling values also show significant dipol-CSA cross-correlated relaxation rates (e.g., R21, D62).[30,44]

We have shown that H−N bond length information and/or backbone order parameters are accessible with high accuracy in a perdeuterated protein. The error in the estimation of the dipolar coupling is as small as 150 Hz, corresponding to a variation of the bond length in the order of ca. 0.005 Å. Perdeuteration is required to avoid $^1H,^1H$ dipolar decoupling during the recoupling period. Effects of rf inhomogeneity are suppressed by using CPPI to reintroduce the $^1H,^{15}N$ dipolar coupling. We find no variation of the N−H bond length as a function of hydrogen bonding (within the error of the experiment). Instead, small $^1H,^{15}N$ dipolar coupling values are found only for amides with small H^N chemical shift values, indicating weak hydrogen bonding and, in turn, increased flexibility for those parts of the protein. We expect that the determination of overall order parameters from high-accuracy $^1H,^{15}N$ dipolar coupling experiments (in addition to ^{15}N T_1 and cross-correlated relaxation experiments) will play an important role in the characterization of backbone motion in the solid state in the future.

Materials and Methods

Sample Preparation. A pET3d derivative coding for α-spectrin SH3 domain from chicken brain was a gift of M. Saraste. Protein was expressed in *Escherichia coli* BL21 (DE3) in M9 minimal medium using 100% D_2O, with 4 g/L of $^2H_8$−glycerol as the sole carbon source, together with 1 g/L of $^{15}N-NH_4Cl$. Cells were grown at 37 °C up to an optical density ($OD_{600\ nm}$) of 0.6. The temperature was then decreased to 22 °C, and induction was started with 1 mM IPTG overnight. Purification of the cell extract was carried out in H_2O-containing buffer systems as reported earlier (anion exchange on a Q-Sepharose FF column, followed by gel filtration on a Superdex75 column).[45] This yielded an amide-protonated, carbon-deuterated preparation. Ten milligrams of that sample was lyophilized and redissolved in H_2O/D_2O using a mixing ratio of 10:90 with respect to solvent exchangeable protons. Microcrystalline precipitates were obtained by mixing the protein solution (10 mg/mL) at a ratio of 1:1 with a 200 mM $(NH_4)_2SO_4$ solution (in 90% D_2O; the pH value was adjusted to around 7 using an alkaline atmosphere).

NMR Spectroscopy. MAS solid-state NMR experiments were performed at a magnetic field strength of 9.4 T, employing a Bruker Avance 400WB spectrometer. The spectrometer was equipped with a standard 3.2-mm triple resonance MAS probe. The MAS rotation frequency was set to 20 kHz in all experiments. The effective temperature was adjusted to 11 °C, using a methanol sample for exact temperature calibration.

The dipolar recoupling scheme relies on the previously introduced phase-inverted CP element in which ^1H and ^{15}N rf fields are simultaneously phase-alternated every 10 μs by 180° while the Hartmann−Hahn matching condition synchronously alternates between the +1 and −1 rotary resonance condition.[37−39] The experiment was recorded in a pseudo three-dimensional fashion in which the $^1H-^{15}N$ dipolar coupling is reintroduced during t_1 (Figure 1). The indirect evolution period t_1 was incremented in steps of 60 μs, comprising six rf field alternations per step. The total number of increments amounted to 84, allowing for a maximum $^1H,^{15}N$ polarization transfer time of 4.98 ms. The incremented CPPI

(43) Case, D. A. *J. Biomol. NMR* **1999**, *15*, 95–102.
(44) Chevelkov, V.; Faelber, K.; Schrey, A.; Rehbein, K.; Diehl, A.; Reif, B. *J. Am. Chem. Soc.* **2007**, *129*, 10195–10200.
(45) Pauli, J.; Van Rossum, B.-J.; Förster, H.; De Groot, H. J. M.; Oschkinat, H. *J. Magn. Reson.* **2000**, *143*, 411–416.

element is preceded by a constant CP step of 60 μs duration, which was applied to minimize the central band artifact and to increase the amplitude of oscillations in t_1 as described previously.[38,39] For CPPI, the rf field on the ^{1}H channel was set to 49 kHz, while the rf field on the ^{15}N channel was alternating between 69 and 29 kHz. The ^{1}H,^{15}N Hartmann−Hahn condition was optimized with high accuracy in a standard CP experiment by iterative adjustment of the rf field strength and the CP contact time in steps of 0.2 dB and 2 μs, respectively. Fast switching of phase and amplitude during CPPI was achieved by implementing CPPI as a shape in XWINNMR.

The ^{1}H,^{15}N correlation (f_2, f_3) following the CPPI building block is required to yield site-specific resolution. The maximum evolution times t_2^{max} and t_3^{max} were set to 57.9 and 66 ms, respectively. All rf hard pulses on the ^{1}H and ^{15}N channel are applied using an rf field of 61.3 and 48.2 kHz, respectively.

The pulse scheme relies on proton detection in the solid state.[46−48] Amide cross-peak assignments are obtained from scalar coupling based 3D triple resonance correlation experiments.[49] Effective suppression of the solvent signal is achieved using a scheme suggested by Zilm and co-workers.[50] After the recoupling step, ^{15}N polarization is stored along the z-axis during a variable delay ($\tau - t_2/2$) that precedes and follows the ^{15}N evolution period t_2. Two delays ($\tau - t_2/2$) are required to allow for a 180° proton pulse for J decoupling in the indirect dimension, keeping the duration of the experiment constant with respect to the water magnetization. The fixed delay τ_w is optimized for water signal suppression and is equal to 100 ms.

Perdeuterated samples do not require proton homonuclear decoupling. Proton−proton dipolar decoupling would introduce a scaling factor in the measurement of the heteronuclear dipolar coupling. As discussed previously,[18,19,38,39] the experimental value for the scaling factor depends on the exact calibration of the ^{1}H rf field, its homogeneity, the offset of the proton chemical shift from the carrier frequency, and an eventual cross-polarization mismatch. This dependence further increases the inaccuracy of the obtained order parameters. In addition, high-power decoupling can introduce heating into the sample,[51] which might result in an overestimation of motional effects. As in deuterated samples decoupling is not an issue, the accuracy of the measurement is potentially improved.

Numerical Simulations. The software package SIMPSON[52] was used to carry out a best fit simulation of the experimental data and to explore the influence of the experimental conditions on the accuracy of the experimental results. Powder averaging was performed using 2000 α and β angle pairs according to the REPULSION scheme,[53] while the number of γ angles was restricted to 10. In the simulations, a reduced anisotropy $\delta_z = \delta_{zz} - \delta_{iso}$ for the nitrogen[54,55] and the proton CSA tensor[56] of 106 and 6.6 ppm was assumed, setting the asymmetry to 0.2 and 0.95, respectively. To extract the dipolar coupling for residue D62, a smaller value for δ_z was assumed (62.6 ppm), taking into account motional averaging (the dipolar coupling is scaled compared to the average dipolar coupling by a factor of 1.7).

Simulations (see Supporting Information) show that variations of the anisotropy of the ^{1}H CSA tensor parameters affect the estimated heteronuclear dipolar coupling by less than 0.2%, which is consistent with other studies.[18,19,38,39] Changes in the asymmetry and orientation of the ^{1}H CSA tensor result in variations of the extracted dipolar coupling on the order of ±0.02%. Variations in the nitrogen isotropic shift (±12.5 ppm) and in the asymmetry parameter ($\eta = 0-0.5$) introduce an inaccuracy of ±0.05%. The finite rf field switching time (0.1 μs) during CPPI results in an error of the extracted dipolar coupling in the order of ±0.01%. The proton isotropic chemical shift and the strength of the applied ^{1}H rf field strength have a significant impact (see Supporting Information) on the simulated ^{1}H,^{15}N dipolar coupling values and were included in all simulations. The error induced by an uncertainty in the nitrogen chemical shift anisotropy and the H−N bond orientation with respect to the principal axis of the nitrogen CSA tensor affect the extracted dipolar coupling values, yielding an error on the order of 1%. A detailed analysis of this effect is given in the Supporting Information.

Acknowledgment. This work was supported by the Leibniz-Gemeinschaft and the DFG (Grants Re1435, SFB 449, SFB 740).

Supporting Information Available: Effect of radio frequency inhomogeneity on the dipolar recoupling spectrum obtained from CP and CPPI; estimation of the experimental error in the determination of the ^{1}H−^{15}N dipolar couplings; influence of the ^{1}H chemical shift offset on the experimental dipolar splitting; dependence of the experimental dipolar splitting D^{app} on the ^{1}H rf field strength employed in the CPPI experiment; dependence of the experimental dipolar splitting D^{app} on the ^{15}N anisotropic chemical shift δ_z and the angle β between the principal axis of the CSA tensor and the ^{1}H−^{15}N dipolar tensor. This material is available free of charge via the Internet at http://pubs.acs.org.

JA902649U

(46) Reif, B.; Jaroniec, C. P.; Rienstra, C. M.; Hohwy, M.; Griffin, R. G. *J. Magn. Reson.* **2001**, *151*, 320–327.
(47) Reif, B.; Griffin, R. G. *J. Magn. Reson.* **2003**, *160*, 78–83.
(48) Chevelkov, V.; van Rossum, B. J.; Castellani, F.; Rehbein, K.; Diehl, A.; Hohwy, M.; Steuernagel, S.; Engelke, F.; Oschkinat, H.; Reif, B. *J. Am. Chem. Soc.* **2003**, *125*, 7788–7789.
(49) Linser, R.; Fink, U.; Reif, B. *J. Magn. Reson.* **2008**, *193*, 89–93.
(50) Paulson, E. K.; Morcombe, C. R.; Gaponenko, V.; Dancheck, B.; Byrd, R. A.; Zilm, K. W. *J. Am. Chem. Soc.* **2003**, *125*, 15831–15836.
(51) Linser, R.; Chevelkov, V.; Diehl, A.; Reif, B. *J. Magn. Reson.* **2007**, *189*, 209–216.
(52) Bak, M.; Rasmussen, J. T.; Nielsen, N. C. *J. Magn. Reson.* **2000**, *147*, 296–330.
(53) Bak, M.; Nielsen, N. C. *J. Magn. Reson.* **1997**, *125*, 132–139.
(54) Wylie, B. J.; Franks, W. T.; Rienstra, C. M. *J. Phys. Chem. B* **2006**, *110*, 10926–10936.
(55) Hiyama, Y.; Niu, C.-H.; Silverton, J. V.; Bavoso, A.; Torchia, D. A. *J. Am. Chem. Soc.* **1988**, *110*, 2378–2383.
(56) Loth, K.; Pelupessy, P.; Bodenhausen, G. *J. Am. Chem. Soc.* **2005**, *127*, 6062–6068.